submitted to *Geophys. J. Int.*

Tests of ocean-tide models by analysis of satellite-to-satellite range measurements: An update

EXPRESS LETTER

R. D. Ray[1], B. D. Loomis[1], S. B. Luthcke[1], and K. E. Rachlin[2]

[1] *Geodesy & Geophysics Laboratory, NASA Goddard Space Flight Center, Greenbelt, MD, USA*

[2] *KBRWyle, Greenbelt, MD, USA.*

SUMMARY

Seven years of GRACE intersatellite range-rate measurements are used to test the new ocean tide model FES2014 and to compare against similar results obtained with earlier models. These qualitative assessments show that FES2014 represents a marked improvement in accuracy over its earlier incarnation, FES2012, with especially notable improvements in the Arctic Ocean for constituents K_1 and S_2. Degradation appears to have occurred in two anomalous regions: the Ross Sea for the O_1 constituent and the Weddell Sea for M_2.

Key words: Tides – Ocean tides – satellite gravity

1 INTRODUCTION

A few years ago Stammer et al. (2014) conducted a suite of comprehensive tests of seven modern altimeter-constrained ocean-tide models. Many of the tests relied on comparisons against *in situ* tidal measurements, but some relied on remote measurements. One of the most valuable remote tests was based on analysis of satellite-to-satellite ranging data from the GRACE satellites (Tapley et al. 2004), using an approach described by Ray et al. (2009). These provided some of the best tests in polar regions, where high-quality *in situ* data are lacking and where the models themselves are least accurate.

The present short note is essentially a footnote to the GRACE analysis described by Stammer et al. (2014), updated now to include a new tidal model that is already being widely adopted in many varied applications.

Subsequent to the Stammer et al. testing work, a new version of the French finite-element model, FES2014, was developed and a large global atlas of constituents has now been publicly released (Carrère et al. 2016). This is the latest in a series of global finite-element models begun by the late C. Le Provost and colleagues (Le Provost et al. 1994) and continuing with refinements in spatial resolution, accuracy, and comprehensiveness (Lyard et al. 2006). The FES2014 atlas, although created on a finite-element grid, has been released on a global (1/16)° latitude-longitude grid, with 34 constituents.

Tests of the FES2014 model done by several groups—some published (Quartly et al. 2017), many unpublished—suggest it represents a clear advance in global modeling. The model has already been adopted for use by some international projects (e.g., Quartly et al. 2017), and it is currently the default ocean-tide model in the widely used Radar Altimeter Database System (Scharroo et al. 2013). Some standard tide-gauge tests, such as those employed by Stammer et al. (2014), are not especially useful in testing this model because many of those data were assimilated into the solution. It is thus timely to subject FES2014 to the same GRACE tests that have been found previously useful, especially for the unique insights GRACE can yield over the polar regions.

Our analysis of the FES2014 tidal model follows exactly the approach used in Section 6.1.2 of Stammer et al. (2014). So the following section only briefly outlines the procedure. This is followed by the main results, which focus on the problematic tides of the polar seas, including the tides under polar ice shelves.

2 METHODOLOGY

We use the Release-2 version of the Level-1B GRACE data generated at the Jet Propulsion Laboratory. The Level-1B datasets contain the fundamental K-band microwave ranging measurements, 3-axis accelerometer measurements, attitude parameters, and GPS-based orbit ephemerides. We used the data from 2004–2010, a period during which active thermal control of both spacecraft was maintained.

The adopted prior models of Earth's time-varying gravity should be as comprehensive as possible in order to isolate the small signals of tidal residuals in the intersatellite range data. Along with high-degree models of the static geopotential, atmospheric mass variations, and glacial isostatic adjustment, we used the MOG2D model (Carrère & Lyard 2003) for non-tidal ocean mass variations. Both the atmospheric and oceanic mass models have 3-hour time resolution, and the former includes the main diurnal and subdiurnal barometric tides. Hydrological and cryospheric mass variations were modeled by using the previous GRACE solutions of Luthcke et al. (2013), which are expressed in terms of

"mascons," or localized mass anomalies. Only terrestrial mascons were used; oceanic mascons were set to zero to prevent possible removal of any correlated tidal signals. Near land/water boundaries it is possible some "cross talk" between hydrological and ocean tidal signals remains, especially for the S_2 constituent whose alias period in GRACE is a relatively long 161 days (Ray et al. 2003).

The ocean tide elevations are expressed in spherical harmonic form, with the major constituents of interest here taken to degree and order 90. For each tested ocean-tide model, we recomputed satellite orbit parameters, allowing initial states to adjust as needed. GRACE's range-rate residuals were then converted to range acceleration residuals, because anomalies in acceleration are better localized over their causative mass anomalies. Acceleration residuals can, however, lead to noticeable side lobes over large anomalies (Ray et al. 2009), something to keep in mind when examining final maps. Our range accelerations were low-pass filtered with a cutoff of approximately 6×10^{-3} Hz. These data were then binned by geographical location and the time series of residuals in each bin subjected to tidal analysis. The end result, for each tested model, is a set of gridded constituents whose amplitudes—still in units of range acceleration—delineate regions of likely tide model error. The results are only a qualitative assessment of model error since they do not yield actual sea-surface elevation errors. To obtain the latter would require an additional inversion step, which is far more expensive computationally and more algorithmically complex, requiring regularization (e.g., Han et al. 2007; Killett et al. 2011) and ultimately assimilation into a hydrodynamical model (Egbert et al. 2009). Although qualitative in nature, and also somewhat "blurry" owing to GRACE's limited spatial resolution, constituent maps of acceleration residuals are still valuable for the unique perspective they give to possible model errors.

3 RESULTS

The main results, which directly compare acceleration residuals of model FES2012 and the newer FES2014, are shown in Figure 1. The two major semidiurnal constituents, M_2 and S_2, and two major diurnal constituents, O_1 and K_1, are shown. Because the GRACE processing has been kept consistent, or nearly consistent, our new maps can be directly compared with similar maps given by Stammer et al. (2014) for several other tide models (HAMTIDE12, OSU12, TPXO.8, EOT11, GOT4.7). Our one inconsistency in processing arises from use of different prior models for terrestrial water storage, which has a very minor effect (mostly in S_2), as can be seen by comparing the previously published maps for model FES2012 with the FES2012 maps shown here.

Figure 1 shows that, for the most part, FES2014 represents a marked improvement over FES2012. In particular, the large FES2012 anomalies in K_1 and S_2 in the Arctic Ocean have been eliminated. In fact, both these constituents are everywhere considerably improved over FES2012. For M_2 and O_1 the changes mostly reflect improvements, but O_1 is noticeably degraded in the Ross Sea area.

As expected, there is little change between latitudes $\pm 66^\circ$, which is an area well constrained by satellite altimetry in both models. Nonetheless, the root-mean-square amplitudes, evaluated over the globe between $\pm 60^\circ$, do show improvement:

O_1:	0.092	0.082 nm s^{-2}
K_1:	0.132	0.119
M_2:	0.250	0.231
S_2:	0.140	0.112

for FES2012 and FES2014, respectively. So the improvements are not limited to only polar regions.

Some lower latitude anomalies clearly remain in M_2, and these are nearly identical in the two models. In fact, they are also nearly identical to M_2 anomalies seen in the other models examined by Stammer et al. (2014), a point noted by those authors. For example, all have small anomalies centered over New Zealand and the southern part of the Patagonian Shelf and relatively large anomalies in the northeast Atlantic. Since these are so similar in all models, we conjecture the problem likely lies with our handling of the GRACE data. Truncation of spherical harmonics at degree 90 conceivably can explain the anomaly over New Zealand, since M_2 is fairly large there but tightly confined as it rotates around the islands. M_2 is also of large amplitude in the northeast Atlantic, so a small scaling error could potentially lead to relatively large observed anomalies. For example, a possible scaling error could arise from errors in the assumed density of seawater, although some initial experiments that adjust the seawater density have not removed the residual anomalies. These problems require follow-up investigation.

Since most of the changes between FES2012 and FES2014 appear in the high latitudes, Figures 2 and 3 serve to better highlight those regions. The FES2014 improvements in K_1 in the Arctic are now especially clear. The O_1 constituent also appears of good quality in the Arctic. Even though the FES2012 solution for O_1 did not have the large problem that occurred in K_1, one can still see small O_1 improvement in the region of Baffin Bay. In the Antarctic figure, both M_2 and K_1 are noticeably improved in the Ross Sea even though O_1 is degraded there. Three of the four constituents are improved in the Weddell Sea, but M_2 is somewhat degraded.

Since polar diagrams were not shown by Stammer et al. (2014), we have also added results from model GOT4.7 (Ray 2013) to Figures 2–3 (these results have again been reprocessed with a terrestrial hydrology model consistent with that used for the two FES models). It is interesting that GOT4.7 displays large anomalies in both diurnal constituents over the Ross Sea, although mainly in the open sea, whereas the anomalies in the FES models are situated more underneath the Ross Ice Shelf. This possibly is due to the use of a small amount of ICESat-1 data in the GOT solutions, but only over the ice shelves, not in the open sea (Ray 2008). Very few ICESat-1 data were available over the Larsen Ice

Shelf, however, in part owing to persistent cloud cover, and O_1 for GOT indeed shows a small anomaly there. GOT also displays evident sidelobes in the diurnal tides north of the Ross Sea, which (as noted above) can happen in range-acceleration residuals when the central anomaly is sufficiently large. The M_2 solution for GOT appears especially poor in the (typically ice-covered) Canadian archipelago, but all models appear inadequate in that region.

While these GRACE results highlight again the well-known problem of model inaccuracies in polar regions, we wish to end on a positive note. While the FES2014 model shows improvements in most polar regions, recent work by Cancet et al. (2018) in the Arctic has yet to be incorporated into FES solutions. Moreover, to our knowledge no global model has yet attempted to use Cryosat-2 altimeter data, yet recent work by Zaron (2018) as well as Cancet et al. (2018) shows good improvements can be obtained with these data over both ice shelves and (partly sea-ice impacted) open ocean. The recently launched ICESat-2 satellite should also lead to more and better data that enables further progress.

ACKNOWLEDGMENTS

This work was funded by the U.S. National Aeronautics and Space Administration through the GRACE science team. The GRACE Level 1B data are available from the Physical Oceanography Distributed Active Archive Center (PODAAC) at the Jet Propulsion Laboratory.

REFERENCES

Cancet, M., Andersen, O. B., Lyard, F., Cotton, D., & Benveniste, J., 2018. Arctide2017, a high-resolution regional tidal model in the Arctic Ocean, *Adv. Space Res.*, **62**, 1324–1343.

Carrère, L. & Lyard, F., 2003. Modeling the barotropic response of the global ocean to atmospheric wind and pressure forcing – comparisons with observations, *Geophys. Res. Lett.*, **30**(6), 1275.

Carrère, L., Lyard, F., Cancet, M., Guillot, A., & Picot, N., 2016. FES2014, a new tidal model: Validation results and perspectives for improvements, Presentation at ESA Living Planet Conference, Prague.

Egbert, G. D., Erofeeva, S. Y., Han, S.-C., Luthcke, S. B., & Ray, R. D., 2009. Assimilation of GRACE tide solutions into a numerical hydrodynamic inverse model, *Geophys. Res. Lett.*, **36**, L20609.

Han, S.-C., Ray, R. D., & Luthcke, S. B., 2007. Ocean tidal solutions in Antarctica from GRACE inter-satellite tracking data, *Geophys. Res. Lett.*, **34**, L21607.

Killett, B., Wahr, J., Desai, S., Yuan, D., & Watkins, M., 2011. Arctic ocean tides from GRACE satellite accelerations, *J. Geophys. Res.*, **116**(C11), C11005.

Le Provost, C., Genco, M. L., Lyard, F., Vincent, P., & Canceil, P., 1994. Spectroscopy of the world ocean tides from a finite element hydrodynamic model, *J. Geophys. Res.*, **99**, 24777–24797.

Luthcke, S. B., Sabaka, T. J., Loomis, B. D., Arendt, A. A., McCarthy, J. J., & Camp, J., 2013. Antarc-

tica, Greenland amd Gulf of Alaska land-ice evolution from an iterated GRACE global mascon solution, *J. Glaciology.*, **59**, 613–631.

Lyard, F., Lefevre, F., Letellier, T., & Francis, O., 2006. Modelling the global ocean tides: modern insights from FES2004, *Ocean Dynam.*, **56**, 394–415.

Quartly, G. D., Legeais, J.-F., Ablain, M., Zawadzki, L., Fernandes, M. J., Rudenki, S., Carrère, L., García, P. N., Cipollini, P., Andersen, O. B., Poisson, J.-C., Njiche, S. M., Cazenave, A., & Benveniste, J., 2017. A new phase in the production of quality-controlled sea level data, *Earth Syst. Sci. Data*, **9**, 557–572.

Ray, R. D., 2008. A preliminary tidal analysis of ICESat laser altimetry: Southern Ross Ice Shelf, *Geophys. Res. Lett.*, **35**, L02505.

Ray, R. D., 2013. Precise comparisons of bottom-pressure and altimetric ocean tides, *J. Geophys. Res. Oceans*, **118**, 4570–4584.

Ray, R. D., Rowlands, D. D., & Egbert, G. D., 2003. Tidal models in a new era of satellite gravimetry, *Space Sci. Rev.*, **108**(1-2), 271–282.

Ray, R. D., Luthcke, S. B., & Boy, J.-P., 2009. Qualitative comparisons of global ocean tide models by analysis of intersatellite ranging data, *J. Geophys. Res.*, **114**, C09017.

Scharroo, R., Leuliette, E. W., Lillibridge, J. L., Byrne, D., Naeije, M. C., & Mitchum, G. T., 2013. RADS: Consistent multi-mission products, in *Proc. Symposium on 20 Years of Progress in Radar Altimetry*, European Space Agency, Spec. Publ. SP-710.

Stammer, D. et al., 2014. Accuracy assessment of global barotropic ocean tide models, *Rev. Geophys.*, **52**, 243–282.

Tapley, B. D., Bettadpur, S., Ries, J. C., Thompson, P. F., & Watkins, M. M., 2004. GRACE measurements of mass variability in the Earth system, *Science*, **305**, 503–505.

Zaron, E. D., 2018. Ocean and ice shelf tides from Cryosat-2 altimetry, *J. Phys. Oceanogr.*, **48**(4), 975–993.

This paper has been produced using the Blackwell Scientific Publications GJI LaTeX2e class file.

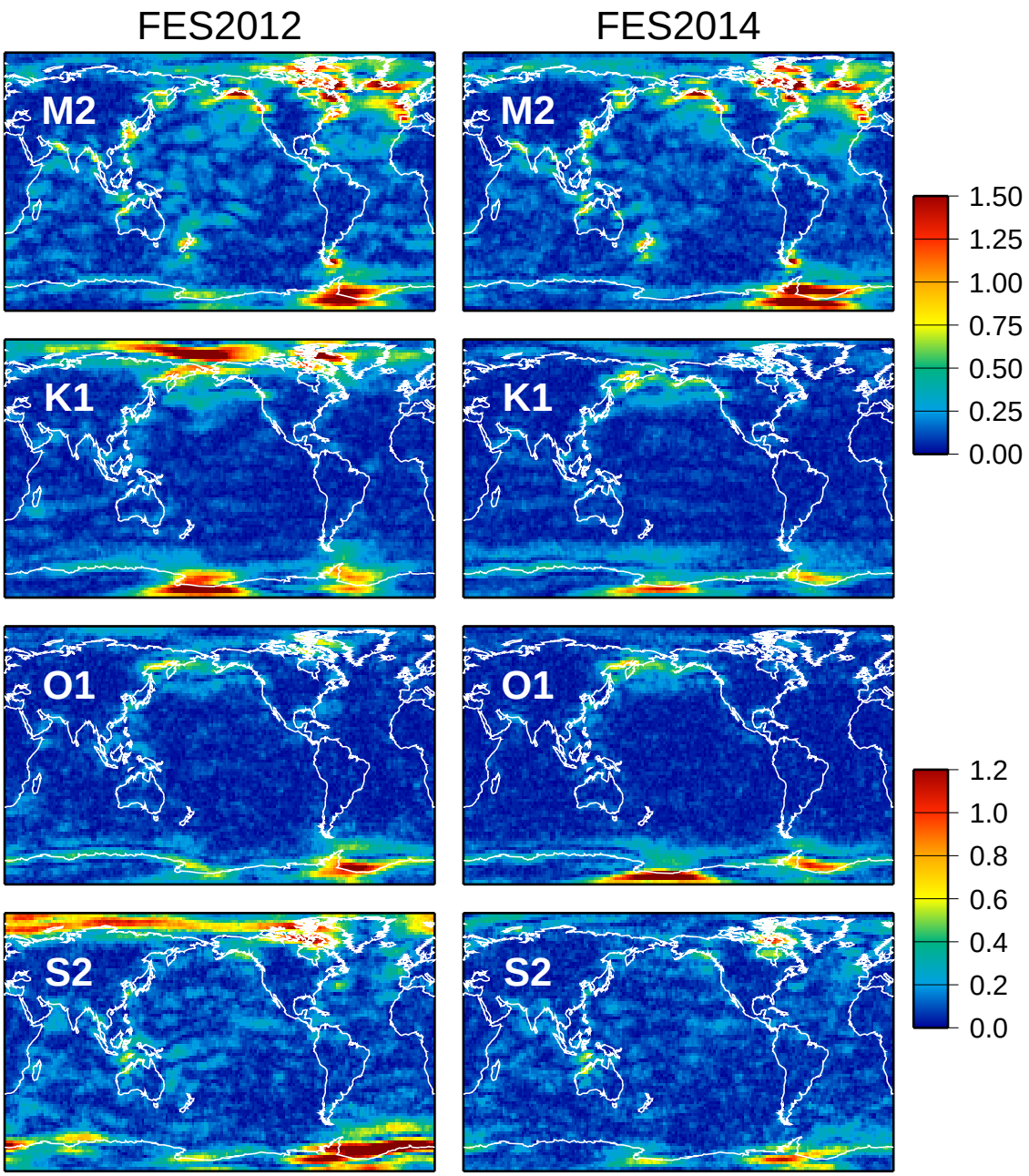

Figure 1. Amplitudes of tidal constituent residuals, in units of nm s^{-2} of GRACE intersatellite range acceleration, based on using either (left) tide model FES2012 or (right) tide model FES2014 to compute the expected tidal perturbation to the intersatellite ranges. Large residual amplitudes occur in places where GRACE's measured ranges disagree with model-based calculated ranges, thus suggesting locations of likely tide model errors.

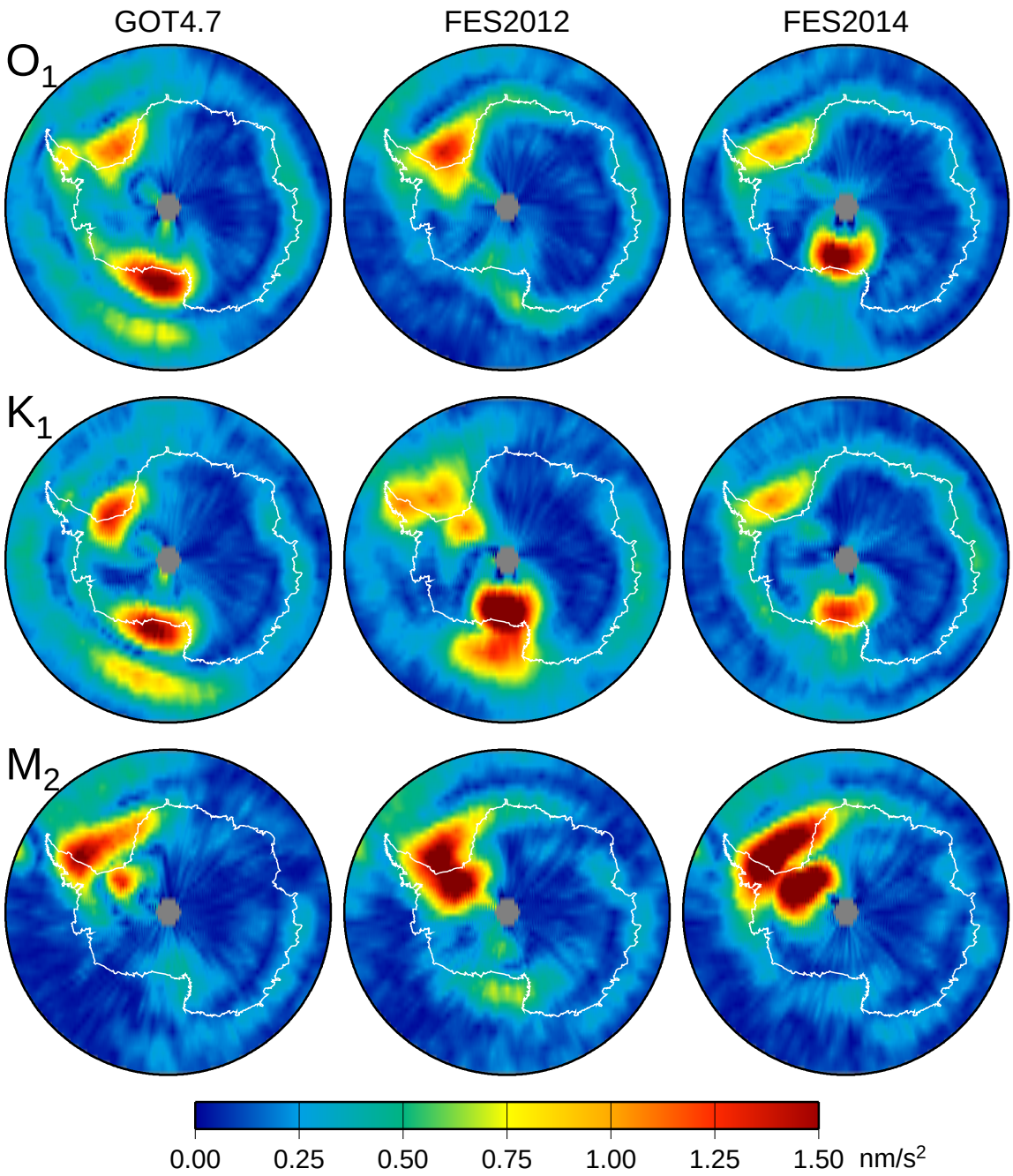

Figure 2. Similar to Figure 1 but for the region south of 60°S. Also shown (leftmost column) are similar results for tide model GOT4.7.

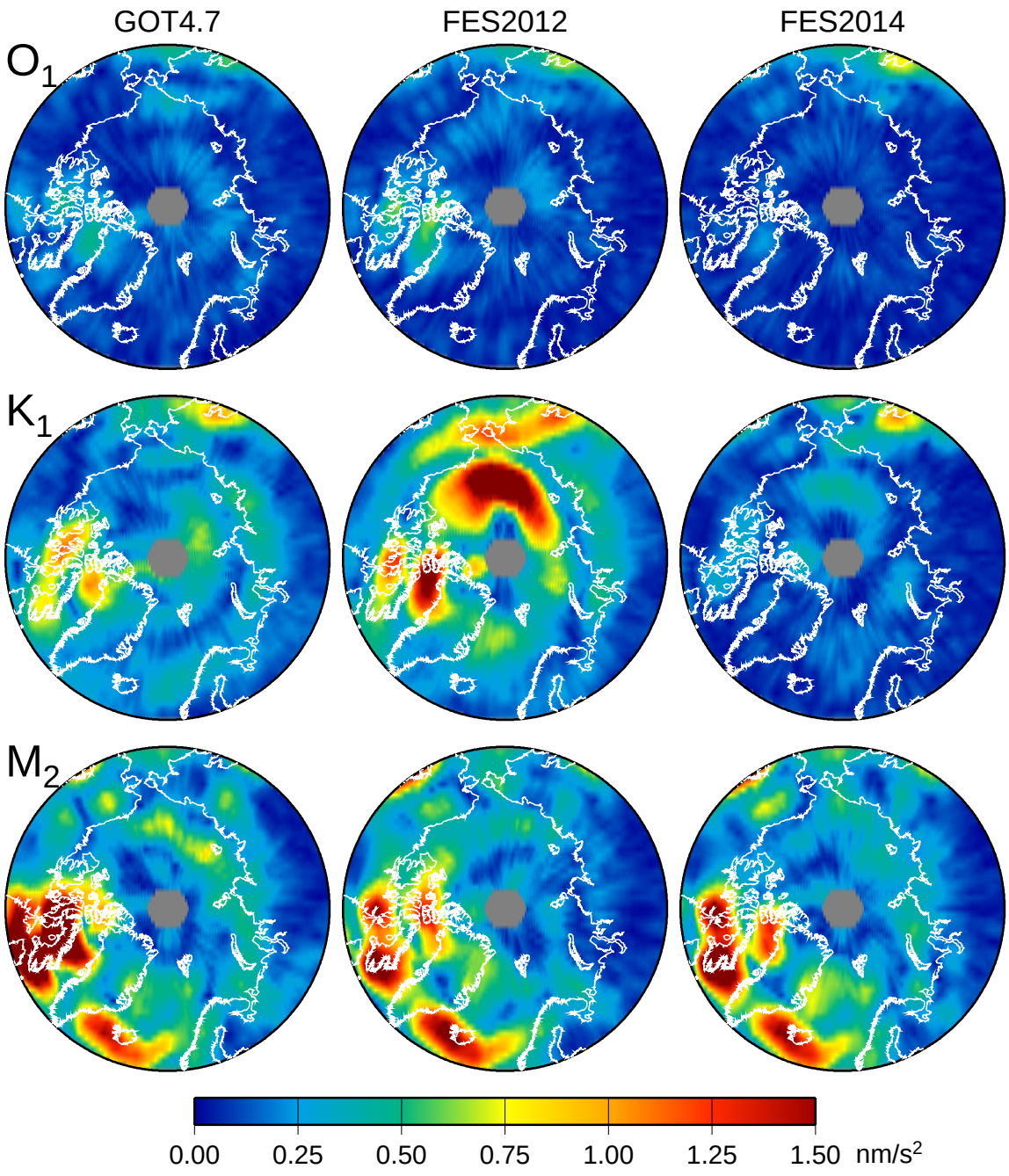

Figure 3. Similar to Figure 1 but for the region north of 60°N.